RSC Advances

ROYAL SOCIETY OF CHEMISTRY

www.rsc.org/advances

Facile synthesis of pure phase γ-AlOOH and γ-Al_2O_3 nanofibers in recoverable ionic liquid via low temperature route

Yuan Cai,[ab] Huihui Huang,[a] Lei Wang,*[a] Xiaojun Zhang,[a] Yuewei Yuan,[a] Rui Li,[a] Hui Wan[a] and Guofeng Guan*[a]

[a] State Key Laboratory of Materials-Oriented Chemical Engineering, College of Chemical Engineering, Nanjing Tech University, Nanjing 210009, PR China. E-mail: guangf@njtech.edu.cn, wanglei@njtech.edu.cn; Tel: +86 25 83587198

[b] Jiangsu Research and Development Center of Chemical Engineering Applying Technology, Department of Chemical Engineering, Nanjing Polytechnic Institute, Nanjing 210048, P.R. China

Abstract

Mesoprous γ-AlOOH and γ-Al_2O_3 with fibrous morphology were successfully synthesized by an ionic liquid ([OMim]Br) assisted low temperature precipitation method using aluminum nitrate and ammonia as aluminum source and precipitant, respectively. The samples were characterized by XRD, TG, FT-IR, TEM, and N_2 adsorption-desorption technique. The results showed that the concentration of [OMim]Br had a significant effect on the phase, porous structures, and morphologies of γ-Al_2O_3 due to the strong interactions between [OMim]Br and γ-AlOOH. High purity γ-AlOOH was synthesized at 0.2 M [OMim]Br and γ-Al_2O_3 with specific surface area of 243.53 m^2/g, pore volume of 0.68 cm^3/g, and average pore size of 11.10 nm was obtained after calcination. Furthermore, the recyclability of [OMim]Br was investigated. The recovery rate of [OMim]Br could reach 95.0wt%, and the recycled [OMim]Br still had effects on the synthesis of γ-AlOOH and γ-Al_2O_3.

1. Introduction

Al_2O_3 is a vital industrial material which has been used in an extensive range of fields, such as catalysis, catalyst support, purification, filler, abrasive, paint and so on. [1-3] Al_2O_3 exists in many forms, α, χ, η, δ, κ, θ, γ, ρ, etc. Among them, γ-Al_2O_3 is the most important one for its widespread applications owing to the specific physicochemical

properties, such as textual properties, acid/base characteristics, morphology and strength.[4] Therefore, the preparation of Al_2O_3 with unique characteristics has received increased attentions. Precipitation method is widely used to synthesize γ-Al_2O_3, in which low temperature precipitation, characterized by lower energy expenditure, is more mild and economical in synthesis process. Aluminum nitrate salt is one of the most common sources of aluminium for preparing precursors of γ-Al_2O_3. However, using low temperature precipitation to prepare precursors of γ-Al_2O_3 from aluminum nitrate salt is prone to obtain the mixed precursors of gibbsite and boehmite(γ-AlOOH).[5, 6] γ-AlOOH is a desirable precursor of γ-Al_2O_3 due to the energy saving with morphology and textual structure preserved.[7, 8] Thus, it is important to investigate the appropriate technology or suitable additives in low temperature precipitation to control the synthesis of γ-AlOOH.

In previous research, the appropriate surfactant has been proven to be an effective approach to synthesis γ-AlOOH and improve its properties.[9] Ionic liquids (ILs), with the properties of wide liquid range, negligible vapor pressure, good thermal stability, and adjustable physical and chemical properties, have been investigated as novel and green media for synthesis materials.[10-14] Particularly, the property of forming extended hydrogen bond systems in the liquid state and reusability favor their application performance.[15, 16] Up to now, various inorganic materials have been prepared using ILs with different approaches. For instance, nanosized metal fluorides have been fabricated in $BMIMBF_4$ ionic liquids solvent has been reported.[17] Titania,[18, 19]iron oxide and Al_2O_3/titania composite have been prepared in ionic liquid.[20, 21] γ-Al_2O_3 nanostructures with various morphologies has been controllably synthesized via ionic-liquids-assisted hydrothermal routes and the effect models of ILs has been found by Zheng' group.[22-24] However, most approaches are hydrothermal or ionothermal routes, which require high temperature, pressure and a large amount of ionic liquids. Hence, it is a challenge to fabricate pure γ-AlOOH and γ-Al_2O_3 and adjust the textual structure with ionic liquids using inorganic aluminum source by low temperature precipitation. In addition, it requires great effort to recycle ionic liquids from the perspective of green chemistry.

In this paper, we report a facile and environmentally friendly route to synthesize fibrous γ-AlOOH and γ-Al_2O_3 with high purity via 1-butyl-3-methylimidazole bromide ([OMim]Br) assisted low temperature precipitation method using inorganic $Al(NO_3)_3 \cdot 9H_2O$ and $NH_3 \cdot H_2O$ as aluminum source and precipitant, respectively. The effects of [OMim]Br concentration on the phase, textual structure, and morphology of γ-AlOOH and γ-Al_2O_3 products are elucidated. In addition, the recyclability of [OMim]Br is highlighted in this paper.

2. Experimental Section

2.1. Materials and preparation

Materials: Aluminum nitrate (A.R.), ammonia (A.R.), absolute ethanol (A.R.), and ethyl acetate (A.R.) were obtained from Sinopharm Chemical Reagent Co., Ltd. N-methylimidazole (A.R.), and 1-Bromooctane (A.R.) were purchased from Aladdin. All of the reagents were used without further purification. Ionic liquid 1-octyl-3-methylimidazole bromide ([OMim]Br) was synthesized according to the Reference.[25]

The synthesis of fibrous γ-Al_2O_3 with [OMim]Br: 0.01 mol $Al(NO_3)_3 \cdot 9H_2O$ and different amounts of [OMim]Br ($C_{[OMim]Br}$ = 0, 0.05, 0.1, 0.2, 0.4 M) were added into 100 mL of deionized water under vigorous stirring to form a homogeneous solution. Then, γ-AlOOH precipitate was formed after ammonia was added into the solution with a feeding rate of 500 μL/min. The pH of the solution was adjusted to pH 8.5, which was monitored by a PHS-2F pH meter. After aging at 55 ^oC for 24 h, the mixture was processed with centrifugation and divided into two layers. The upper layer was the mixture of ionic liquid [OMim]Br and H_2O and the lower layer was the precipitate of precursor γ-Al_2O_3 (γ-AlOOH), which was washed with deionized water and ethanol and dried under vacuum at 60 ^oC for 12 h. The upper layer and the washed residual liquids were processed with vacuum distillation and then ionic liquid [OMim]Br was recovered. γ-Al_2O_3 was obtained after γ-AlOOH was calcinated at 600 ^oC for 6 h.

2.2. Characterization

The XRD was performed on a Philips X'pert MPD Pro diffractometer equipped with Ni-filtered Cu Kα radiation (λ=0.15418 nm). FT-IR spectra were collected on a

Thermo Nicolet 870 spectrophotometer with a resolution of $5cm^{-1}$ using anhydrous KBr as dispersing agent. The thermogravimetric (TG) and differential scanning calorimetry (DSC) were conducted with use of a Netzsch STA 449F3 simultaneous DSC-TG thermogravimetric analyzer. N_2 adsorption-desorption measurements were carried out on a Micromeritics ASAP 2020 system model instrument at 77 K. The specific surface area was calculated by the Brunauer-Emmett-Teller (BET) algorithm. The mesoporous pore size distribution was obtained using the Barrett-Joyner-Halenda (BJH) theory. TEM images were obtained with a JEOL (model 794) instrument employing an acceleration voltage of 120 kV.

3. Results and Discussion

3.1 Characterization of γ-AlOOH and γ-Al_2O_3

The phase and purity of samples are characterized by XRD. The precursors synthesized without/with [OMim]Br are shown in Figure 1(A). The broad diffraction peaks of the as-synthesized samples reveal their nanoscale nature. In the absence of [OMim]Br, the precursor can be mainly indexed as γ-AlOOH (JCPDS 21-1307) and the weak diffraction peaks observed at 20^o, 40^o and 53^o correspond to the $Al(OH)_3$ impurity phase (JCPDS 77-0114). The intensities of $Al(OH)_3$ diffraction peaks firstly become stronger then weaker by increasing the concentration of [OMim]Br from 0 to 0.05 M then to 0.1M. However, the diffraction peaks of $Al(OH)_3$ disappear for the sample synthesized at $C_{[OMim]Br}$ = 0.2, 0.4 M, indicating the complete phase transformation from $Al(OH)_3$ to AlOOH. Figure 1(B) presents XRD patterns of all alumina after calcination at 600 ^oC. The alumina is mainly amorphous without [OMim]Br. While all alumina, synthesized in the presence of [OMim]Br, can be assigned to γ-Al_2O_3 (JCPDS 10-0425). The weak intensity and broad bands indicate the low crystallinity of γ-Al_2O_3.

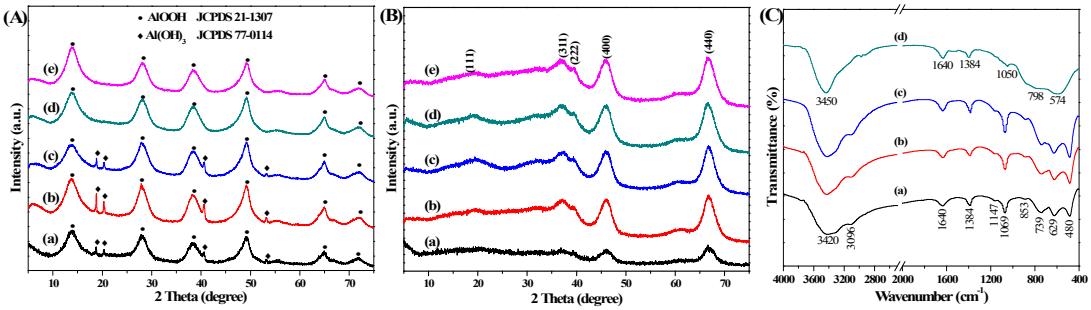

Figure 1. XRD patterns of the as-synthesized precursors (A) and corresponding γ-Al_2O_3 (B) at varying $C_{[OMim]Br}$ = 0 (a), 0.05 (b), 0.1 (c), 0.2 (d), 0.4 M (e); FT-IR spectra (C) of as-synthesized precursors at varying $C_{[OMim]Br}$ = 0 (a), 0.05 (b), 0.2 (c) and Al_2O_3 synthesized at $C_{[OMim]Br}$ = 0.2 M (d).

To further confirm the chemical compositions of as-synthesized precursor and alumina, FT-IR measurement is carried out in the region of 400-4000 cm^{-1}. In the FT-IR spectra (Figure 1(C)) of as-synthesized samples, two broad bands at 3420 and 3096 cm^{-1} belong to the ν_{as}(Al)–OH and ν_s(Al)O–H stretching vibrations of γ-AlOOH. In the spectra of γ-AlOOH synthesized at $C_{[OMim]Br}$ = 0.2 M, the weak bands at 2949 and 2866 cm^{-1} due to the asymmetric and symmetric CH_2 stretch respectively, are detectable. This result demonstrates trace amount of [OMim]Br is still in γ-AlOOH though the sample has been washed for several times. These phenomena may be related to the hydrogen bond between [OMim]Br and -OH in γ-AlOOH. Another sharp peak at 1069 cm^{-1} and the weak shoulder at 1147 cm^{-1} are assigned to the δ_sAl–O–H and δ_{as}Al–O–H bending vibrations of γ-AlOOH, respectively. The three bands at 739, 629 and 480 cm^{-1} represent the vibration mode of [AlO_6], while the 853 cm^{-1} structure results from the stretching of [AlO_4] atomic group. The above bands are typical features of γ-AlOOH,[13, 26] which are consistent with XRD results. The weak band at 1640 cm^{-1} is attributed to the bending vibration band of adsorbed water. After calcination, the bands at 543 cm^{-1} and 798 cm^{-1} were assigned to [AlO_4] and [AlO_6] sites in γ-Al_2O_3.[27, 28] The broad bands around 3450 and 1640 cm^{-1} show the existence of -OH.

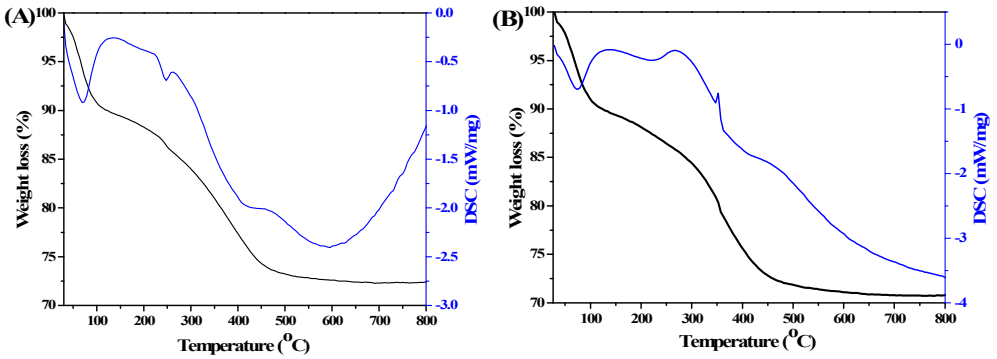

Figure 2. TG-DSC curves of as-synthesized precursors synthesized at $C_{[OMim]Br}$ =0 (a), 0.2 M (b).

Thermal stabilities of as-synthesized precursors without/with [OMim]Br are studied by thermogravimetry-differential scanning calorimetry (TG-DSC). Typical TG-DSC curves of as-syntesized samples synthesized at $C_{[OMim]Br}$ = 0, 0.2 M are shown in Figure 2. The initial weight loss from 25 °C to 150 °C, accompanied with an endothermal peak around 75 °C in the DSC curves, can be assigned to the removal of physical adsorbed water. The second weight loss from 150 °C to 450 °C, with an endothermic peak around 250 °C, is due to the first stage of dehydration by condensation of Al-OH groups. The last region of weight loss in the region of 450-800 °C is associated with a second stage of dehydration by the condensation of hydroxyl groups.[29] However, compared with the DSC curves of sample synthesized at $C_{[OMim]Br}$ =0, there is an additional exothermic peak around 350 °C in the DSC curves synthesized at $C_{[OMim]Br}$ = 0.2 M, which can be attributed to the decomposition of [OMim]Br. The weight loss at 150 °C and 450 °C is 15.1 wt% and 16.7 wt%, respectively. However, the theoretical weight loss of the phase transition from γ-AlOOH to Al_2O_3 is 15 wt%, which means the actual weight loss of samples synthesized at $C_{[OMim]Br}$ = 0.2 M is higher than the theoretical value. The extra mass loss (1.7 wt%) can be ascribed to the decomposition of [OMim]Br.

The effect of adding the [OMim]Br in the formation of γ-Al_2O_3 is analyzed by N_2 adsorption-desorption. For N_2 adsorption-desorption isotherms in Figure 3(A), all isotherms are classified as type IV, according to the International Union of Pure and Applied Chemistry (IUPAC) classification,[30] verifying they are mesoporous materials. When the relative pressure is between 0.6 and 1, the isotherms of γ-Al_2O_3 synthesized

at $C_{[OMim]Br}$ =0, 0.05, 0.1, 0.2 M show H1-type hysteresis loops, as shown in Figure 3(A). However, the isotherm of γ-Al_2O_3 synthesized at $C_{[OMim]Br}$ = 0.4 M exhibits H_2-type hysteresis loops, indicating interconnected pore network. Figure 3(B) shows the pore size distributions of all γ-Al_2O_3, calculated from the desorption data of isotherms using the Barrett-Joyner-Halenda (BJH) method. All γ-Al_2O_3 are featured with bimodal mesoporous distribution in the range of 5-20 nm. The texture properties of γ-Al_2O_3 products, the BET specific surface area, pore volume and the average pore size, are summarized in Table 1. The γ-Al_2O_3 synthesized at $C_{[OMim]Br}$ = 0.1 M presents the highest BET surface area (258.02 m^2/g) and the highest pore volume (0.78 cm^3/g) with an average pore diameter of 12.13 nm. The γ-Al_2O_3 with specific surface area of 243.53 m^2/g, pore volume of 0.68 cm^3/g, and average pore size of 11.10 nm was obtained after the calcination of high purity γ-AlOOH, which was synthesized at 0.2 M [OMim]Br. It is interesting that the influence of [OMim]Br on the texture properties of γ-Al_2O_3 products shows an evident trend. As shown in Figure 3(C-E), the BET specific surface area, pore volume and the average pore size of these γ-Al_2O_3 products exhibit a linear trend which firstly increases and then decreases with increasing [OMim]Br. Therefore, we can handily control the textual structure of Al_2O_3 by adjusting the concentration of [OMim]Br.

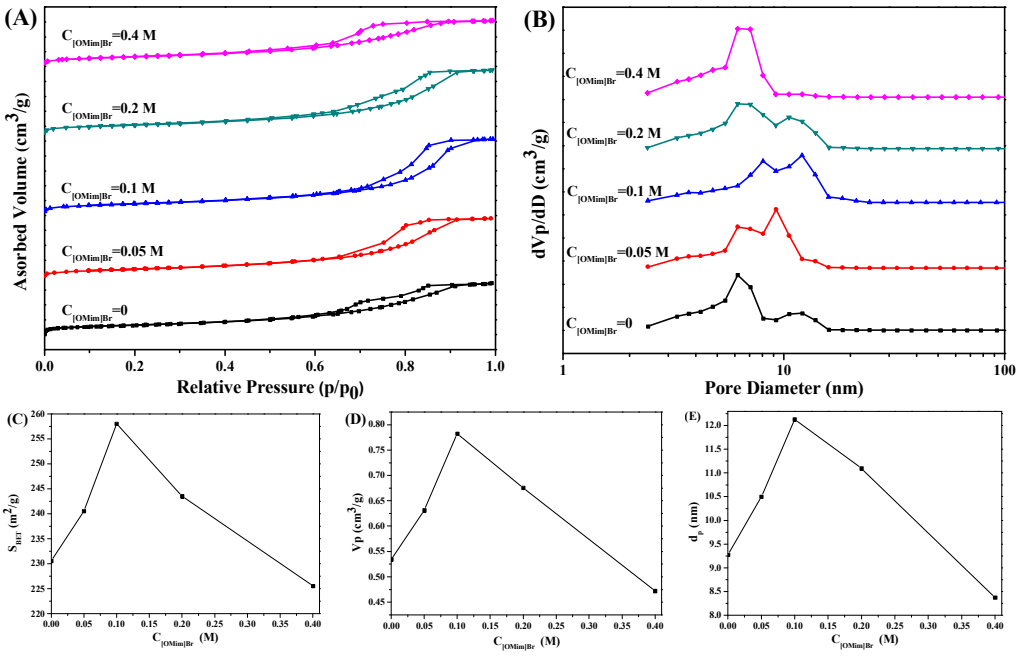

Figure 3. (A) N_2 adsorption-desorption isotherms, (B) BJH pore-size distribution and (C) BET specific surface area, (D) pore volume and (E) average pore size changes of γ-Al_2O_3 with varying $C_{[OMim]Br}$.

The morphology of γ-Al_2O_3 synthesized at $C_{[OMim]Br}$ =0 and 0.2 M is observed by transmission electron microscopy. The sample synthesized without [OMim]Br contains some fibers and particles with irregular morphology. However, the γ-Al_2O_3 synthesized at $C_{[OMim]Br}$ = 0.2 M consists mainly of fibers, which are relatively more uniform than that at $C_{[OMim]Br}$ = 0. Furthermore, the sample is composed of flocculence-like mesostructures as previous report.[31] As shown in Fig. 4(b), the fiber, with the length of 20-30 nm, width 2-3 nm, is composed of many small crystalline nanosized particles with interconnected pores. The selected area electron diffraction (SAED) pattern (inset in Figure 4(a)) of the nanofibers confirms the crystal structure with γ-Al_2O_3 phase, which is consistent with the results of XRD.

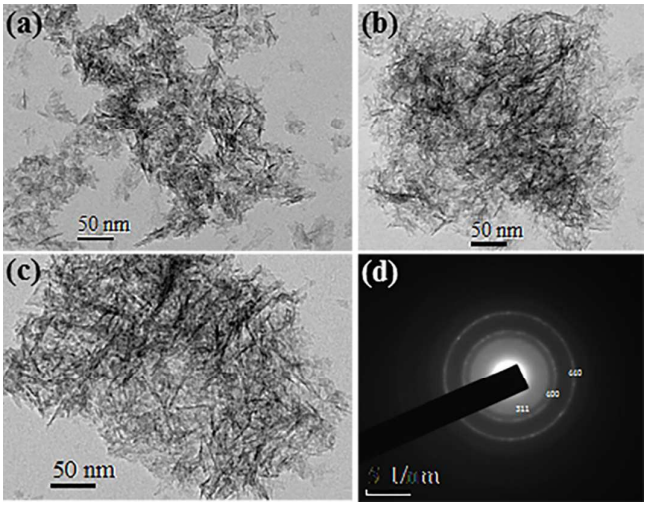

Figure 4. TEM images of γ-Al_2O_3 synthesized at $C_{[OMim]Br}$ = 0 (a), 0.2 M (b) and 0.4 M (c) and corresponding SAED pattern of γ-Al_2O_3 synthesized at $C_{[OMim]Br}$ =0.2 M (d).

Results of the morphologies of γ-Al_2O_3 with different templates were investigated, which were listed in Table 1. The morphology of γ-Al_2O_3 is greatly affected by the templates, and varies from nanosheets, hollow urchin, rod to flower under different templates. As shown in Table 1, the specific surface area of nanofibers γ-Al_2O_3 prepared by ionic liquid ([OMim]Br) assisted low temperature precipitation in this paper is higher than that synthesized via other ionic liquids assisted method in

previous reports, and is similar with that prepared by conventional templates.

Table 1. The comparison of morphology of γ-Al_2O_3 with different templates

	Reaction conditions				Morphology	Specific surface area/(m^2 g^{-1})	Ref.
	Temperature/℃	Time/h	Solution	Template			
1	430-450	192	DI water	SiO_2	Nanosheets	21.40	[32]
2	100	24	DI water	P123	Amorphous	182.00	[5]
3	120	24	DI water	TX-100	Hollow urchin	146.91	[9]
4	100	48	DI water	PEO	Nanofibers	347.40	[33]
5	25-30	24	Ethanol	[Bmim]PF_6	Rod	85.00	[34]
6	170	36	DI water	[OMim]Cl	Flower	164.60	[35]
7	55	24	DI water	[OMim]Br	Nanofibers	258.02	This work

3.2 The effect of [OMim]Br

According to the above results, [OMim]Br leads to changes of the phase, morphology and pore structure. A possible formation mechanism of γ-AlOOH nanofibers is proposed as shown in Scheme 1. [OMim]Br is a solvent and template, widely used in the synthesis of inorganic materials. When it is in aqueous solution, it can mix with water in all compositions and form micelles.[36, 37] In this system, [OMim]Br can easily adsorb onto the surface of AlOOH particles to form aligned hydrogen bonds and additional π-π interactions[12]. Thus, the surface energy of aluminum oxyhydroxide can be reduced. The aluminum oxyhydroxide is more stable with [OMim]Br than that without [OMim]Br, inducing well-grown nanofibers. At the same time, due to the long side-chain on the imidazole ring, the bulky molecules prevent the aggregation effectively. With increasing [OMim]Br, more [OMim]Br molecules adsorb on the surface of particles, the growth predominance of nanofibers increases.

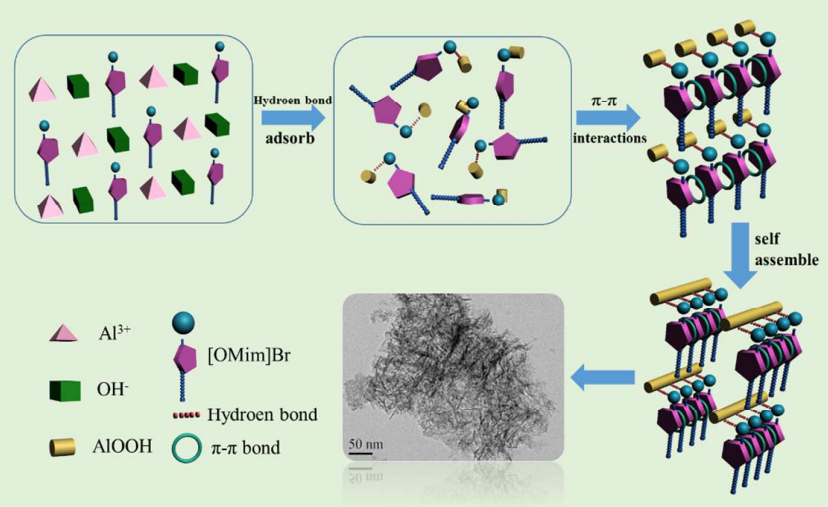

Scheme 1. The schematic demonstration of the formation process of γ-AlOOH.

In addition, the increase by the addition of [OMim]Br gives rise to the viscosity of the system. The viscosity of the system and the aggregation of [OMim]Br micelles increases quickly with increasing [OMim]Br, which will suppress the access of [OMim]Br to aluminum oxyhydroxide causing the decrease in the textual parameter of alumina, namely the "viscosity-controlled" mechanism.[38] However, with the concentration of [OMim]Br increases and ultimately reaches 0.2 M, the number of the [OMim]Br molecules is increasing. The distribution of [OMim]Br is not uniform, some [OMim]Br may not adsorb on the surface of aluminum oxyhydroxide and the crystallites of aluminum oxyhydroxide aggregate together and form particles.

3.3 The recyclability of [OMim]Br

Though ILs do not release harmful gases into the atmosphere because of the low volatility, they may become waste liquor causing unpredictable water and/or land contamination for their inaccessible biodegradability. In addition, the price of ILs is relatively high in comparison with other general templates employed in synthesis of inorganic materials. Therefore, the recycling of ILs plays an important role in the green chemistry and economics theory of inorganic materials synthesis.

To investigate the recyclability of [OMim]Br, the [OMim]Br was used for 5 runs and recycled by available vacuum distillation. Moreover, it is noteworthy that the recovery rate of [OMim]Br could reach as high as 95.0wt%, the remaining 5.0wt%

loss might include the loss in the reaction process and precursor. The recycled [OMim]Br is further applied into resynthesizing the AlOOH and Al_2O_3. And the result of γ-Al_2O_3 with $C_{[OMim]Br}$ = 0.2 M after washed by water and ethanol, dried and calcined is shown in Figure 5. From Figure 5, it can be seen that using recycled [OMim]Br we can also obtain γ-AlOOH (JCPDS 21-1307) and γ-Al_2O_3 (JCPDS 10-0425). The obtained γ-Al_2O_3 has mesoporous structure with type IV N_2 adsorption-desorption isotherm further characterized by N_2 adsorption-desorption. The textual parameters of obtained γ-Al_2O_3 are respectively BET surface area 278.96 m^2/g, pore volume 0.97 cm^3/g and average pore diameter of 13.6 nm. In addition, as shown in the TEM image, the morphology of obtained γ-Al_2O_3 is also fibrous. In summary, the similar fibrous γ-Al_2O_3 can be produced with mesoporous structure using recycled [Omim]Br by simple recovery process. Effects of the recycled [OMim]Br on the synthesis of γ-AlOOH were almost the same as those of the fresh [OMim]Br.

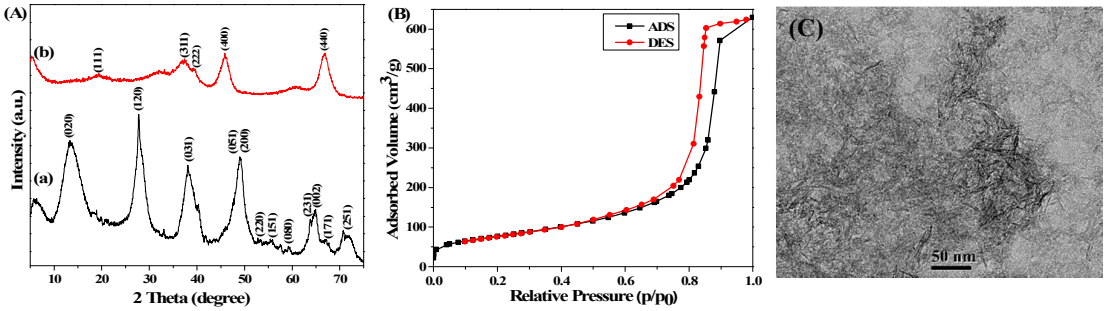

Figure 5. (A)XRD patterns: as-synthesized AlOOH (a) and γ-Al_2O_3 (b); (B) N_2 adsorption-desorption isotherm and (C)TEM images of γ-Al_2O_3 synthesized at $C_{[OMim]Br}$ = 0.2 M with recycled [OMim]Br for 5 times.

4. Conclusions

In summary, we have successfully synthesized γ-AlOOH and γ-Al_2O_3 with fiber morphology by [OMim]Br assisted low temperature precipitation method. Based on results of characterizations, the concentration of [OMim]Br affects the phase of γ-AlOOH and the optional concentration of [OMim]Br is 0.2 M at which γ-AlOOH with high purity can be obtained. After calcination, γ-Al_2O_3 is obtained with the specific surface area of 243.53 m^2/g, pore volume of 0.68 cm^3/g and average pore size

of 11.10 nm. All of them firstly increase then decrease with the increasing concentration of [OMim]Br with 0.1 M as the critical point, which makes it possible to precisely control the synthesis of γ-Al_2O_3 with specific textual properties. Furthermore, the recyclability of [OMim]Br has been investigated. The recovery rate of [OMim]Br could reach 95.0wt% and the recycled [OMim]Br had effects on the γ-Al_2O_3. The recyclability of [OMim]Br may have a promising potential in the field of inorganic materials synthesis.

Acknowledgements

This work was financially supported by the National Natural Science Foundation of China (no. 21176121, no. 21306082), the Natural Science Foundation of the Jiangsu Higher Education Institutions of China (12KJB530004), and the Foundation from State Key Laboratory of Materials-Oriented Chemical Engineering, Nanjing Tech University (ZK201305).

References:

1. B. Maleki and S. S. Ashrafi, *RSC Adv.*, 2014, 4, 42873-42891.
2. Z. Salam, E. Vijayakumar and A. Subramania, *RSC Adv.*, 2014, 4, 52871-52877.
3. X. F. Shang, X. G. Wang, W. X. Nie, X. F. Guo, X. J. Zou, W. Z. Ding and X. G. Lu, *J. Mater. Chem.*, 2012, 22, 23806-23814.
4. M. Trueba and S. P. Trasatti, *Eur. J. Inorg. Chem.*, 2005, 36, 3393-3403.
5. P. Bai, P. P. Wu, Z. F. Yan and X. S. Zhao, *J. Mater. Chem*, 2009, 19, 1554-1563.
6. D. Mishra, S. Anand, R. K. Panda and R. P. Das, *Mater. Lett.*, 2002, 53, 133-137.
7. A. Malki, Z. Mekhalif, S. Detriche, G. Fonder, A. Boumaza and A. Djelloul, *J. Solid State Chem.*, 2014, 215, 8-15.
8. A. D. V. Souza, C. C. Arruda, L. Fernandes, M. L. P. Antunes, P. K. Kiyohara and R. Salomão, *J. Eur. Ceram. Soc.*, 2015, 35, 803-812.
9. H. H. Huang, L. Wang, Y. Cai, C. C. Zhou, Y. W. Yuan, X. J. Zhang, H. Wan and G. F. Guan, *Crystengcomm*, 2015, 17, 1318-1325.
10. R. D. Rogers and K. R. Seddon, *Science*, 2003, 302, 792-793.
11. Z. S. Qureshi, K. M. Deshmukh and B. M. Bhanage, *Clean Technol. Envir.*, 2014, 16, 1487-1513.
12. L. Xu, J. X. Xia, H. Xu, S. Yin, K. Wang, L. Y. Huang, L. G. Wang and H. M. Li, *J. Power Sources*, 2014, 245, 866-874.
13. Z. H. Li, Z. Jia, Y. X. Luan and T. C. Mu, *Curr. Opin. Solid St. M.*, 2008, 12, 1-8.
14. H. Wan, C. Chen, Z. W. Wu, Y. G. Que, Y. Feng, W. Wang, L. Wang, G. F. Guan and X. Q. Liu, *ChemCatChem*, 2015, 7, 441-449.
15. M. Antonietti, D. B. Kuang, B. Smarsly and Z. Yong, *Angew. Chem. Int. Edit.*, 2004, 43,

4988-4992.

16. Y. Zhou, *Curr. Nanosci.*, 2005, 1, 35-42.

17. D. S. Jacob, L. Bitton, J. Grinblat, I. Felner, Y. Koltypin and A. Gedanken, *Chem. Mater.*, 2006, 18, 3162-3168.

18. H. Choi, J. K. Yong, R. S. Varma and D. D. Dionysiou, *Chem. Mater.*, 2006, 18, 5377-5384.

19. Y. Zhou and M. Antonietti, *J. Am. Chem. Soc.*, 2003, 125, 14960-14961.

20. H. K. Farag, M. A. Zoubi and F. Endres, *J. Mater. Sci.*, 2009, 44, 122-128.

21. P. Shikha, B. S. Randhawa and T. S. Kang, *RSC Adv.*, 2015, 5, 51158-51168.

22. T. Kim, J. B. Lian, J. M. Ma, X. C. Duan and W. J. Zheng, *Cryst. Growth Des.*, 2010, 10, 2928-2933.

23. T. Kim, H. B. Li, J. B. Lian, H. H. Jin, J. M. Ma, X. C. Duan, G. Yao and W. J. Zheng, *Cryst. Res. Technol.*, 2010, 45, 767-770.

24. X. C. Duan, T. Kim, D. Li, J. M. Ma and W. J. Zheng, *Chem. - Eur. J.*, 2013, 19, 5924-5937.

25. L. T. B. Thi, W. Korth, S. Aschauer and A. Jess, *Green Chem.*, 2009, 11, 1961-1967.

26. A. Boumaza, L. Favaro, J. Lédion, G. Sattonnay, J. B. Brubach, P. Berthet, A. M. Huntz, P. Roy and R. Tétot, *J. Solid State Chem.*, 2009, 182, 1171-1176.

27. D. M. Ibrahim and Y. M. Abu-Ayana, *Mater. Chem. Phys.*, 2009, 113, 579-586.

28. K. M. Parida, A. C. Pradhan, J. Das and N. Sahu, *Mater. Chem. Phys.*, 2009, 113, 244-248.

29. J. J. Fitzgerald, G. Piedra, S. F. Dec, M. Seger and G. E. Maciel, *J. Am. Chem. Soc.*, 1997, 119, 7832-7842.

30. K. S. W. Sing, D. H. Everett, R. A. W. Haul, L. Moscou, R. A. Pierotti, J. Rouquerol and T. Siemieniewska, *Pure Appl. Chem.*, 1985, 11, 603-619.

31. Z. Liu and C. Lv, *RSC Adv.*, 2014, 4, 10221-10227.

32. W. L. Suchanek and J. M. Garcés, *Crystengcomm*, 2010, 12, 2996-3002.

33. H. Y. Zhu, J. D. Riches and J. C. Barry, *Chem. Mater.*, 2002, 14, 2086-2093.

34. X. W. Ji, S. K. Tang, L. Gu, T. C. Liu and X. W. Zhang, *Mater. Lett.*, 2015, 151, 20-23.

35. Z. Tang, J. L. Liang, X. H. Li, J. F. Li, H. L. Guo, Y. Q. Liu and C. G. Liu, *J. Solid State Chem.*, 2013, 202, 305-314.

36. J. P. Hallett and T. Welton, *Chem. Rev.*, 2011, 111, 3508-3576.

37. A. Modaressi, H. Sifaoui, M. Mielcarz, U. Domańska and M. Rogalski, *Colloids and Surfaces a: Physicochemical and Engineering Aspects*, 2007, 302, 181-185.

38. Z. Tang, X. F. Hu, J. L. Liang, J. C. Zhao, Y. Q. Liu and C. G. Liu, *Mater. Res. Bull.*, 2013, 48, 2351-2360.